Current Biology 21, 1748–1755, October 25, 2011 ©2011 Elsevier Ltd All rights reserved DOI 10.1016/j.cub.2011.09.008

Report

Emergent Growth Cone Responses to Combinations of Slit1 and Netrin 1 in Thalamocortical Axon Topography

Franck Bielle,[1,2,3,6] Paula Marcos-Mondéjar,[4,6] Eduardo Leyva-Díaz,[4,6] Ludmilla Lokmane,[1,2,3,6] Erik Mire,[4] Caroline Mailhes,[1,2,3] Maryama Keita,[1,2,3] Noelia García,[4] Marc Tessier-Lavigne,[5] Sonia Garel,[1,2,3,7,*] and Guillermina López-Bendito[4,7,*]

[1]INSERM, U1024, Avenir Team, 75005 Paris, France
[2]CNRS, UMR 8197, 75005 Paris, France
[3]Ecole Normale Supérieure, Institut de Biologie, IBENS, 46 Rue d'Ulm, 75005 Paris, France
[4]Instituto de Neurociencias de Alicante, Universidad Miguel Hernández-Consejo Superior de Investigaciones Científicas (UMH-CSIC), 03550 Sant Joan d'Alacant, Spain
[5]Genentech, Inc., South San Francisco, CA 94080, USA

Summary

How guidance cues are integrated during the formation of complex axonal tracts remains largely unknown. Thalamocortical axons (TCAs), which convey sensory and motor information to the neocortex, have a rostrocaudal topographic organization initially established within the ventral telencephalon [1–3]. Here, we show that this topography is set in a small hub, the corridor, which contains matching rostrocaudal gradients of Slit1 and Netrin 1. Using in vitro and in vivo experiments, we show that Slit1 is a rostral repellent that positions intermediate axons. For rostral axons, although Slit1 is also repulsive and Netrin 1 has no chemotactic activity, the two factors combined generate attraction. These results show that Slit1 has a dual context-dependent role in TCA pathfinding and furthermore reveal that a combination of cues produces an emergent activity that neither of them has alone. Our study thus provides a novel framework to explain how a limited set of guidance cues can generate a vast diversity of axonal responses necessary for proper wiring of the nervous system.

Results and Discussion

The functioning of the nervous system relies on the establishment of axonal tracts that follow complex trajectories. Past studies have led to the identification of cues that guide axons toward their targets, such as netrins, semaphorins, ephrins, and Slits. However, it remains unclear how the precise spatial positioning of axonal tracts is achieved in vivo. Thalamocortical projections, which represent the main input to the neocortex and are essential to its functioning, constitute a powerful system to address this issue. Thalamic neurons are spatially organized into distinct nuclei but initially extend their axons in a compact axonal bundle [1]. In the ventral telencephalon or subpallium, thalamocortical axons (TCAs) spread out and acquire a precise rostrocaudal position before their arrival to the neocortex. This topographic positioning ensures that TCAs conveying different sensory and motor information are targeted toward distinct neocortical areas [2, 3]. During their subpallial journey, TCAs first navigate through a permissive corridor generated by tangential cell migration [4] and subsequently cross the striatum. Studies have shown that the initial topographic positioning of TCAs is controlled by information in the subpallium, and more specifically in the striatum [5–7]: gradients of Ephrin A5, Semaphorin 3A (Sema3A), and Sema3F prevent the caudal growth of rostral and intermediate TCAs, respectively [8, 9], while a gradient of Netrin 1 (Ntn1) has been shown to attract rostral axons and repel caudal axons [10, 11]. However, TCAs first travel through the corridor, raising the possibility that it may not only channel all axons internally [4, 12] but also provide positional information for distinct TCAs.

The Corridor: A Decision Point for the Subpallial Topography of TCAs

To address this issue, we first examined where in the subpallium distinct TCAs diverge along the rostrocaudal axis. Using DiA/DiI thalamic injections in a plane of section that encompasses the trajectory of all TCAs (45° corridor slices), we observed that TCAs originating from the caudolateral and rostromedial thalamus adopt a distinct rostrocaudal distribution as they cross the corridor (Figures 1A–1B′). To next determine whether the corridor is instructive for TCA topography, we examined whether modifying the corridor orientation ex vivo affects the rostrocaudal positioning of axons. We focused on rostral (Th1/2) and intermediate (Th3) axons (Figure 1C), which reliably grow along unique directions within the subpallium of organotypic slices as they do in vivo [10, 13]. To manipulate the corridor, we took advantage of an enhancer located between *Dlx5* and *Dlx6* genes (*I56ii*) that drives *LacZ* expression in corridor cells, among other brain structures [14, 15] (see Figure S1 available online). Using this transgenic mouse line (*co-LacZ*), we visualized the corridor using a fluorogenic β-galactosidase substrate and performed rostrocaudal flipping of the corridor or control incisions in 45° slices (Figure 1D), without affecting or including the adjacent striatum (Figure S1). As expected, when controls slices were cocultured with thalamic explants from *Gfp*-expressing embryos, the majority of Th1/2 TCAs grew rostrally, whereas Th3 TCAs grew at rostrointermediate levels (Figures 1E, 1G, 1H, and 1J). In contrast, after flipping of the corridor, we observed a statistically significant change in axonal behaviors. More specifically, although 20% of the slices were unaffected by the procedure, 80% of the slices showed an inversion of the axonal outgrowth pattern: the majority of Th1/2 and Th3 axons grew at caudal and caudointermediate levels, respectively (Figures 1F, 1G, 1I, and 1J). Collectively, these experiments indicate that the corridor acts upstream of the striatum as a hub for the positioning of rostral and intermediate TCAs.

Slit1 Acts as a Rostral Repellent to Position Intermediate TCAs

To investigate the molecular basis underlying this activity, we searched for guidance cues expressed by corridor neurons.

[6]These authors contributed equally to this work
[7]These authors contributed equally to this work
*Correspondence: garel@biologie.ens.fr (S.G.), g.lbendito@umh.es (G.L.-B.)

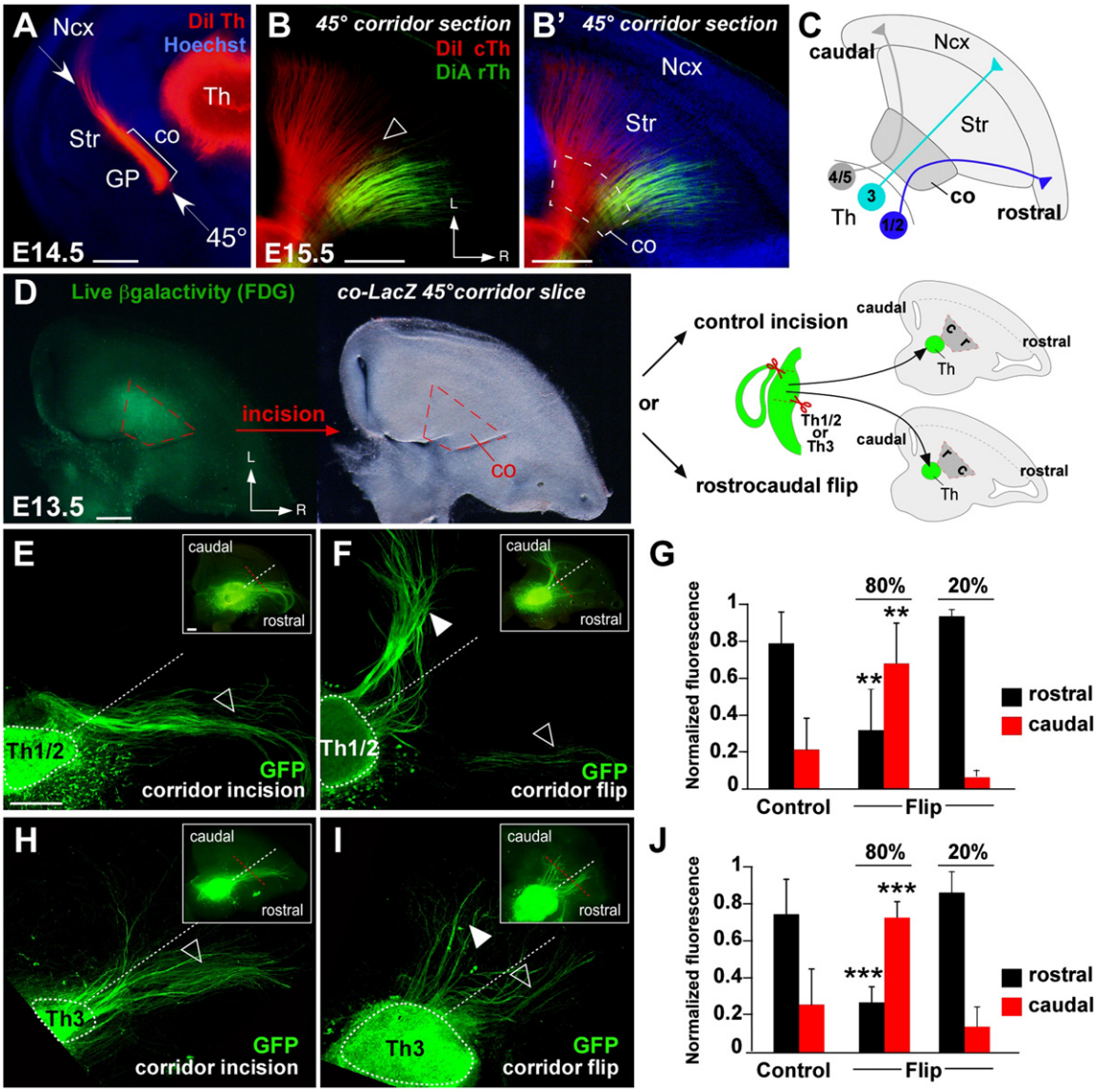

Figure 1. The Corridor Is a Guidance Decision Point for Thalamocortical Axon Topography

(A) Coronal section of an E14.5 brain after DiI injection in the thalamus (Th) shows that labeled thalamocortical axons (TCAs) in the subpallium are encompassed within a 45° plane of section (45° corridor angle), which is used in the following panels.

(B and B′) 45° corridor angle sections after DiI and DiA injections at E15.5 in the caudolateral (cTh) and rostromedial thalamus (rTh) show distinct positioning of caudal (red, DiI) and rostral (green, DiA) axons (arrowhead) within the corridor (dotted line).

(C) Schema of the topographical arrangement of TCAs in the corridor.

(D) Experimental paradigm used to test the presence of guidance information in the corridor. The corridor (co, red dotted line) was transiently labeled on 45° *co-LacZ* E13.5 live sections using a fluorescent substrate of β-galactosidase activity and subsequently cut for a control incision or a rostrocaudal flip. Thalamic (Th) explants of either rostral (Th1/2) or intermediate (Th3) levels from a *Gfp* transgenic mouse were then grafted at the tip of the corridor.

(E and F) Th1/2 grow rostrally (black arrowhead) in controls but mostly caudally (white arrowhead) after the corridor flip [$n(Th1/2)_{control} = 9$; $n(Th1/2)_{flip} = 10$]. Dotted lines indicate the explants and the boundary delineating rostral and caudal quadrants (see Supplemental Experimental Procedures). Inserts show low-magnification images of the entire slices where the red dotted line indicates the corridor/striatum boundary.

(G) Quantification of (E) and (F). **$p < 0.005$ by Student's t test.

(H and I) Th3 grow rostrointermediate in the controls (black arrowhead) but caudointermediate after the corridor flip [$n(Th3)_{control} = 8$; $n(Th3)_{flip} = 9$]. Dotted lines indicate the explants and the boundary delineating rostral and caudal quadrants (see Supplemental Experimental Procedures). Inserts show low-magnification images of the entire slices where the red dotted line indicates the corridor/striatum boundary.

(J) Quantification of (H) and (I). ***$p < 0.001$ by Student's t test.

The following abbreviations are used: c, caudal; L, lateral; Ncx, neocortex; Str, striatum; GP, globus pallidus; r/R, rostral. Scale bars represent 250 μm. Data in (G) and (J) are presented as mean ± standard error of the mean (SEM).

We observed that *ephrinA5* [8], *Sema3A* [9], and *Ntn1* [10, 11] are expressed in the corridor along gradients in register with those described in the striatum: low^{rostral}-high^{caudal} for *ephrinA5* and *Sema3A* and high^{rostral}-low^{caudal} for *Ntn1* (Figure S2). We furthermore found that the secreted factor *Slit1*, in contrast to the closely related *Slit2*, is expressed in the corridor at relatively low levels in addition to its previously characterized expression sites [16, 17] (Figures 2A and 2A′).

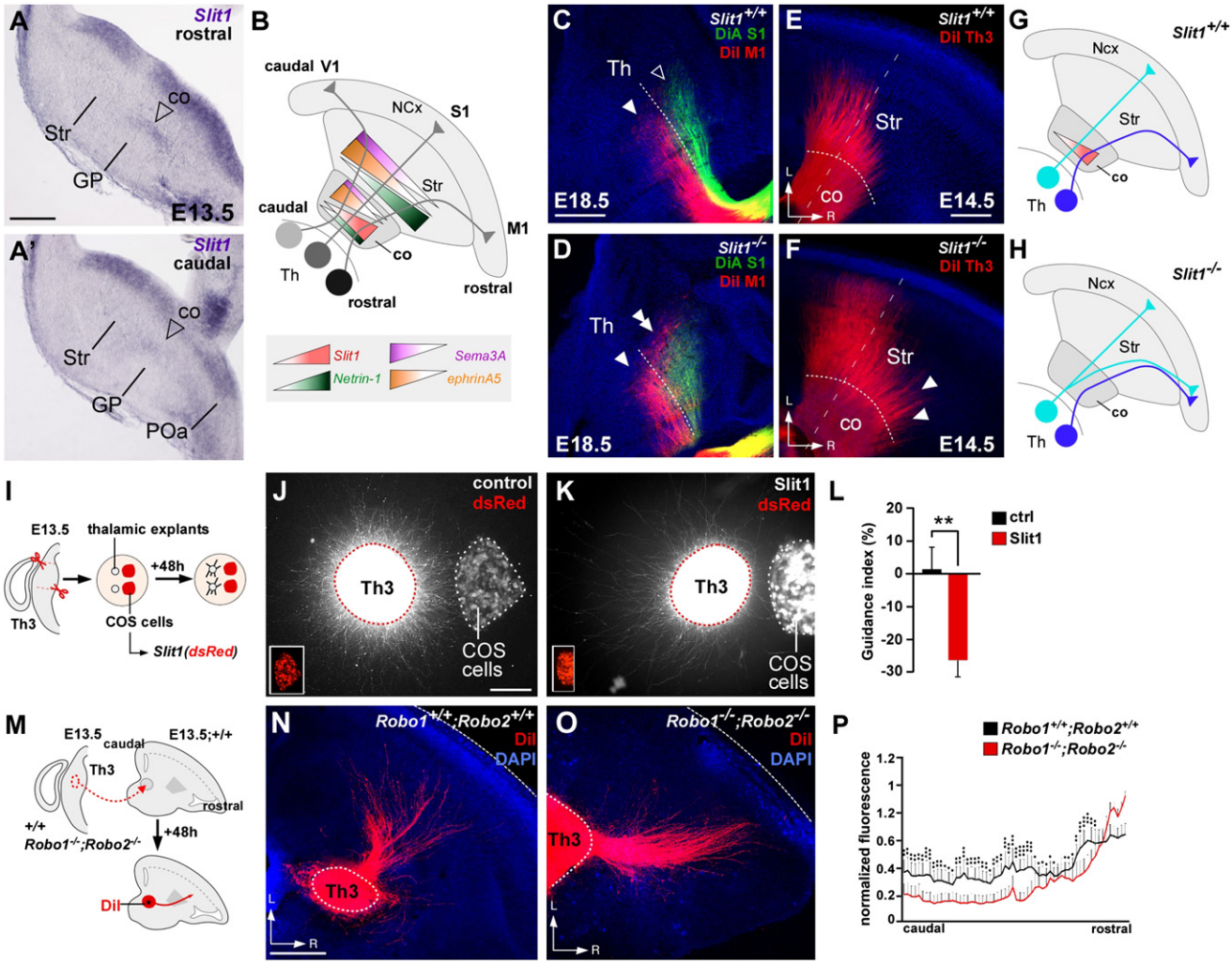

Figure 2. *Slit1* in the Rostral Corridor Positions Intermediate TCAs by Exerting a Repulsive Activity

(A and A′) In situ hybridization on coronal sections showing *Slit1* expression in the corridor (arrowhead) at E13.5 with higher expression at rostral levels (A) than at caudal ones (A′).

(B) Schema representing gradients of guidance molecules in the corridor and the striatum in relationship with the trajectory of TCAs.

(C and D) Coronal hemisections after DiI (red) and DiA (green) labeling from the frontal rostral and parietal intermediate cortex, respectively, at E18.5 in wild-type (C; n = 10) and *Slit1*$^{-/-}$ (D; n = 6) embryos show back-labeled neurons projecting rostrally (white arrowheads) and intermediate (black arrowheads). Some intermediate thalamic neurons are abnormally labeled by frontal injections in *Slit1*$^{-/-}$ (double white arrowhead in D).

(E and F) Anterograde tracing from intermediate thalamus in *Slit1*$^{+/+}$ (E) and *Slit1*$^{-/-}$ (F) showing the rostral dispersion of intermediate axons (arrowheads) in the absence of Slit1. The dotted white lines indicate the corridor/striatum boundary.

(G and H) Schemas representing the trajectory of TCAs in control (G) and *Slit1*$^{-/-}$ (H) embryos.

(I) Experimental procedure to test the activity of Slit1 on Th3 TCAs. Th3 explants were cut from E13.5 embryo sections and confronted in collagen to COS cell aggregates coexpressing *Slit1* and *dsRed* or control cells expressing *dsRed*.

(J and K) Th3 axons grow symmetrically when confronted to control *dsRed*-expressing COS cells (J; n = 17) but are repelled by *Slit1*-expressing COS cells (K; n = 19).

(L) Quantification of the data represented in (J) and (K). **p < 0.005 by Student's t test. The guidance index (see Supplemental Experimental Procedures) allows a graphical representation of axonal responses: positive values indicate attraction, and negative values indicate repulsion.

(M) Experimental paradigm to test the role of Slit/Robo signaling in the topography of intermediate TCAs. Th3 explants were cut from E13.5 wild-type or *Robo1*$^{-/-}$;*Robo2*$^{-/-}$ embryos and cocultured with wild-type 45° sections of the ventral telencephalon.

(N and O) Wild-type Th3 TCAs grow intermediate in the ventral telencephalon (N; n = 10), whereas *Robo1*$^{-/-}$;*Robo2*$^{-/-}$ Th3 axons grow more rostrally (O; n = 9).

(P) Quantification of (N) and (O). *p < 0.05, **p < 0.005, ***p < 0.001 by two-way analysis of variance (ANOVA).

The following abbreviations are used: co, corridor; GP, globus pallidus; M1, primary motor area; S1, primary somatosensory area; Ncx, neocortex; POa, preoptic area; Str, striatum; Th, thalamus. Scale bars represent 250 μm in (A)–(G) and 200 μm in (J), (K), (N), and (O). Data in (L) and (P) are presented as mean ± SEM.

Slit3 might also be expressed in the corridor, albeit at very low levels (data not shown). Because *Slit1* showed higher expression in the rostral corridor and no expression in the striatum, it was a prime candidate for a corridor-specific role in TCA positioning (Figures 2A–2B).

To test the function of *Slit1* on TCA positioning in the corridor, we examined *Slit1*$^{-/-}$ mutant embryos, which have very limited brain development abnormalities [16, 18, 19] and no visible alterations in the subpallium or thalamus patterning (Figure S2; data not shown). To investigate TCA targeting in

Slit1$^{-/-}$ mutants, we first performed DiI and DiA injections at E18.5 in the rostral frontal cortex (motor area, M1) and intermediate parietal cortex (somatosensory area, S1), respectively (Figures 2C and 2D). We observed that both injections back-labeled neurons in the same thalamic nuclei in *Slit1*$^{-/-}$ mutants as in controls (Figure 2C, 2D, 2G, and 2H). However, frontal injections additionally back-labeled neurons in a thalamic nucleus that normally projects to intermediate cortical areas (Figures 2D and 2H), thereby revealing that some intermediate TCAs abnormally reached the rostral cortex in the mutants. By performing DiI anterograde labeling from the intermediate thalamus at E14.5, we found that this rostral misrouting of intermediate TCA occurs as they navigate through the corridor (Figures 2E and 2F).

These observations suggested that Slit1 may act as a rostral corridor repellent for intermediate axons, in agreement with the previous findings that TCAs express the Slit receptors Robo1 and Robo2 and are repelled by Slit2 [20, 21]. Using a coculture assay in collagen matrix, we confirmed that Slit1 repels Th3 axons (Figures 2I–2L). To directly test whether Slit/Robo signaling is required for Th3 axon positioning in the subpallium, we performed cocultures using *Robo1*$^{-/-}$*;Robo2*$^{-/-}$ double-mutant thalamic explants (Figure 2M). Indeed, *Robo1*$^{-/-}$*; Robo2*$^{-/-}$ mutants show major corridor formation defects, thereby precluding an in vivo analysis of TCA topography [12], but have no visible alterations in thalamus patterning (data not shown). We observed that whereas wild-type Th3 TCAs navigate at rostrointermediate levels in the subpallium, a larger proportion of Th3 *Robo1*$^{-/-}$*;Robo2*$^{-/-}$ TCAs grew rostrally (Figures 2N–2P). Overall, our results show that *Slit1* expression in the rostral corridor controls the initial topography of intermediate TCAs by exerting a repulsive activity.

Emergent Combinatorial Activities of Slit1 and Netrin 1 on Rostral TCAs

Because rostral TCAs also express Robo1 and Robo2 receptors [20], the fact that they navigate through the region of higher *Slit1* expression was intriguing (Figure 2B). Indeed, we observed that Slit1 exerts a strong repulsive activity on the growth of Th1/2 axons in collagen assays (Figures 3A–3C). These observations raised the possibility that another factor, absent in vitro, might cooperate to allow the positioning of these rostral axons in vivo. Several previous experiments have revealed that Slits can interact with Ntn1 signaling [22–24], in particular for silencing Ntn1-mediated attraction during midline crossing [22]. Because *Ntn1* follows a similar gradient of expression as *Slit1* in the corridor (Figure 2B), we thus wondered whether, in a reverse manner, Ntn1 could override Slit1 repulsion to allow the rostral growth of Th1/2 axons. To this end, we tested the combined effect of Ntn1 and Slit1 activity on the growth of Th1/2 thalamic explants, by confronting them to aggregates of *Slit1*-expressing COS cells mixed with either control cells or *Ntn1*-expressing COS cells in increasing dilutions (1:3, 1:5, and 1:10; Figures 3A–3E). This procedure allowed us to change the relative levels of the two proteins, as indicated by western blot analysis (Figure S3). We observed that increasing concentrations of COS cells secreting Ntn1 were able to abolish Slit1 repulsion starting at a 1:5 dilution (Figures 3B and 3D) and that a further dilution (1:10) induced an attractive activity on Th1/2 axons (Figures 3B and 3E). These results show that Ntn1 can override the repulsion mediated by Slit1 when the levels of Slit1 are moderate compared to Ntn1 levels, as those observed in the rostral corridor in vivo. Furthermore, we observed that the combination of the two factors switched Th1/2 response from repulsion to attraction, consistent with the fact that Ntn1 has been reported to be attractive [10]. However, although *Ntn1*-expressing cells robustly attracted control spinal cord axons (Figure S3; [25]), we surprisingly found that Ntn1 alone has no significant chemotactic activity on E14.5 or E13.5 Th1/2 explants at various concentrations (Figures 3F–3H; Figure S3). These results suggest that the attractive activity of Ntn1 previously detected ex vivo might be partially induced by other factors present in the telencephalon. More importantly, they reveal that when Slit1 and Ntn1 are presented together, an attractive activity that neither of the cues possesses alone emerges from their combination.

These surprising observations could be due to at least two nonexclusive mechanisms: Slit1 mediates attraction in the presence of Ntn1, or Slit1 enables Ntn1 attraction. To distinguish these two possibilities, we performed collagen assays in which aggregates of transfected COS cells provided a focal source of either Ntn1 or Slit1 and increasing doses of recombinant Slit1 (rSlit1) or Ntn1 (rNtn1) were respectively added to the media (Figures 3I and 3J; data not shown). When Slit1 was expressed in COS cells and rNtn1 in the medium, we did not observe an attractive activity on Th1/2 TCAs (data not shown). In contrast, starting at a concentration of 2.5 nM, rSlit1 induced a strong attraction toward the source of Ntn1 (Figures 3G–3J). These observations indicate that a threshold concentration of Slit1 enables Ntn1-mediated attraction of Th1/2 axons. Although our results are consistent with a described role of Slits as potential context-dependent modulators of Ntn1 function in other tracts [22–24], they reveal a strikingly novel interplay between Slit1 and Ntn1 activities on rostral TCAs. Finally, while Slit1 and Ntn1 alone had similar effects on Th3 and Th1/2 explants, their attractive combinatorial activity was never observed on Th3 axons (Figure S3).

The distinct response of rostral and intermediate axons to the Slit1/Ntn1 combination could be due to the presence of different receptors and/or coreceptors on their growth cones. However, whereas Robo3 is not expressed in the thalamus (data not shown), Robo1, Robo2, and the Ntn1 receptors DCC and at least UNC5A/B are present on both Th1/2 and Th3 axons (Figure S3), and their expression is not visibly changed in *Slit1*$^{-/-}$ or *Robo1*$^{-/-}$*;Robo2*$^{-/-}$ mutant embryos (Figure S3; data not shown). Thus, the Th1/2-specific effect of the Slit1/Ntn1 combination cannot be easily explained by a major differential expression of receptors and might rely on interactions between receptors or signaling pathways. To directly test the effect of the two guidance cues on the growth cones of Th1/2 axons, we performed turning assays using acute application of rNtn1 and rSlit1 proteins alone or in combination [26, 27]. Whereas rNtn1 alone had no significant effect (Figures 3K and 3M; Movie S1) and rSlit1 alone induced a repulsive response (Figures 3L and 3M; Movie S2), the combination of the two proteins triggered growth cone turning toward the pipette (Figures 3L and 3M; Movie S3). Thus, the respective activities of Slit1, Ntn1, and their combination that we observed on explants are also found during turning assays of individual growth cones observed by time-lapse microscopy. Altogether, our results show that the relative levels of Slit1 and Ntn1 rapidly trigger a panel of responses in rostral axons that range from repulsion to no effect to attraction.

To test whether in our system the two cues can act in combination to attract rostral axons, we first performed coculture experiments in 45° corridor slices in which an exogenous source of Ntn1 was grafted in the intermediate subpallium in the absence or presence of rSlit1 (Figure 4A). Whereas the

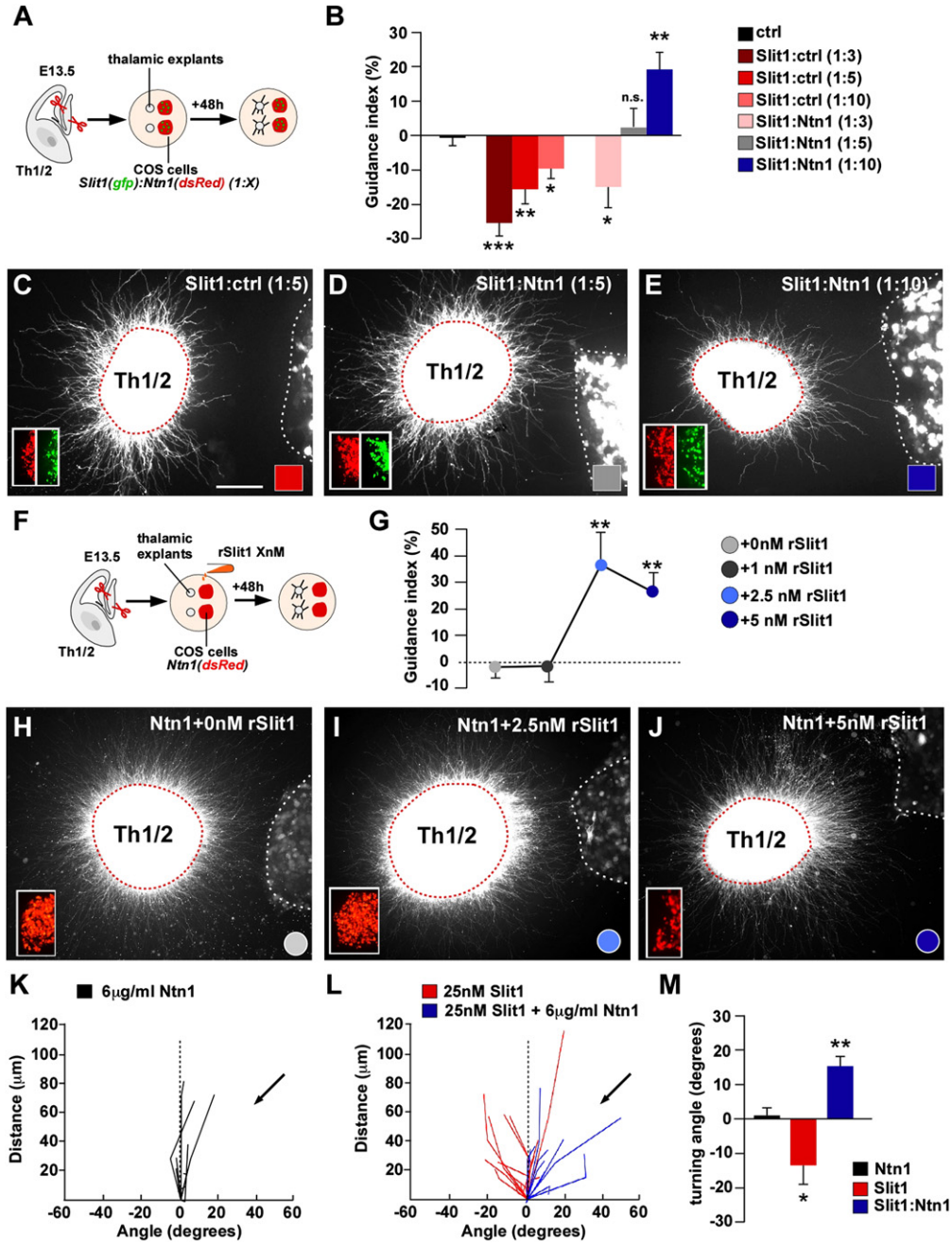

Figure 3. An Emergent Property of Slit1 and Ntn1 Combination on Rostral TCAs

(A) Experimental procedure to test the activity of the combination of Ntn1 and Slit1 on Th1/2 axons. Th1/2 explants were confronted in a collagen matrix to aggregates of COS cells made of mixture in a 1:3, 1:5, or 1:10 dilution ratio between COS cells coexpressing *Slit1/Gfp* and either COS cells expressing *dsRed* or COS cells coexpressing *Ntn1/dsRed*.

(B) Quantification of (C)–(E) and data not shown. *p < 0.05, **p < 0.005, ***p < 0.001 versus controls by Student's t test.

(C) Th1/2 axons are repelled when confronted to COS cells expressing *Slit1/Gfp* and *dsRed* (control) in 1:5 dilution (n = 16 explants). Inserts in the lower left corner show dsRed and GFP expression, respectively, in the COS cell aggregates.

(D) Th1/2 axons show a symmetrical outgrowth when confronted to COS cells expressing *Slit1* and *Ntn1* in a 1:5 dilution (n = 16 explants).

(E) Th1/2 axons are attracted when confronted to COS cells expressing *Slit1* and *Ntn1* in a 1:10 dilution (n = 52 explants).

(F) Experimental procedure to test the effect of Slit1 in Ntn1 response. Th1/2 explants were confronted to COS cell aggregates expressing *Ntn1* and *dsRed* in collagen. Recombinant Slit1 (rSlit1) protein was added to the medium at 0 (n = 37), 1 (n = 24), 2.5 (n = 23), or 5 nM (n = 32) concentration.

(G) Dose-response curve of the data presented in (H)–(J) and data not shown. **p < 0.005 in respect the 0 nM rSlit1 condition by Student's t test.

(H–J) Increasing the concentration of rSlit1 changes the response to Ntn1 from neutral (H) to attraction (I and J).

(K and L) Representative behavior of Th1/2 axons confronted to gradients of guidance cues in turning assays. For each imaged axon, position of the growth cone center was plotted at each time with respect to its position at time 0. Rostral axons have a neutral trajectory in response to Ntn1 (K; n = 12 axons) and are repelled by Slit1 (L; n = 21 axons), whereas Ntn1 and Slit1 trigger an attraction toward the pipette (L; n = 18 axons).

(M) Mean turning angle for all selected axons, shown for each condition. *p < 0.05, **p < 0.01 by Student's t test.

Scale bar in (C) represents 300 μm. Data in (B), (G), and (M) are presented as mean ± SEM.

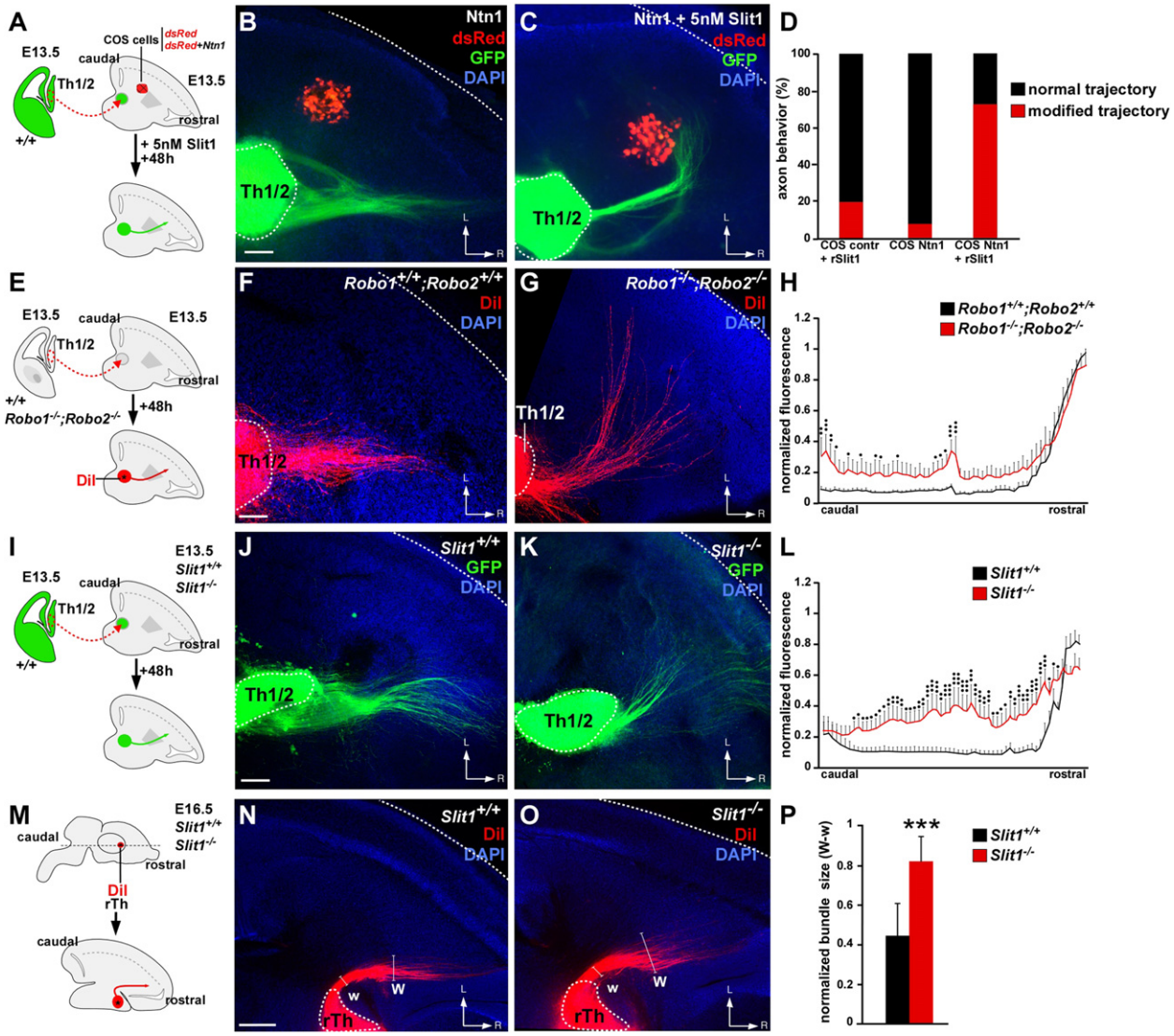

Figure 4. Slit/Robo Signaling Is Necessary for the Channeling of Rostral Axons

(A) Experimental paradigm to test the role of Netrin 1 on the position of rostral axons in the absence or presence of Slit1. Th1/2 explants were cut from E13.5 embryos and cocultured with 45° corridor sections in which a source of *Ntn1*-expressing COS cells was presented in the ventral telencephalon and cultured in the absence or presence of rSlit1 protein.

(B and C) Th1/2 axons deviate toward *Ntn1*-expressing COS cells in the presence of rSlit1 in the medium (C; n = 16 of 22), but not when Ntn1 is present alone (B; n = 2 of 12) or in control COS cells in the presence of rSlit1 (n = 3 of 15).

(D) Quantification of (B) and (C) showing the percentage of slices with a modified trajectory.

(E) Experimental paradigm to test the role of Robo signaling in the guidance of rostral axons. Th1/2 explants were cut from E13.5 wild-type or $Robo1^{-/-}$;$Robo2^{-/-}$ embryos and cocultured with wild-type 45° sections of the ventral telencephalon.

(F and G) Wild-type Th1/2 axons grow rostrally in the subpallium (F; n = 10), whereas some $Robo1^{-/-}$;$Robo2^{-/-}$ Th1/2 axons grow more intermediate (G; n = 9). Dotted lines indicate the borders of the explants and of the receiving slice.

(H) Quantification of (F) and (G). *p < 0.05, **p < 0.005, ***p < 0.001 by two-way ANOVA.

(I) Experimental paradigm to test the role of Slit1 in the navigation of rostral TCAs. Th1/2 explants were cut from E13.5 GFP mouse embryos and cocultured with wild-type or $Slit1^{-/-}$ 45° sections of the ventral telencephalon.

(J and K) Wild-type Th1/2 axons grow rostrally in the ventral telencephalon of wild-type embryos (J; n = 8), whereas some axons grow more intermediate in $Slit1^{-/-}$ slices (K; n = 10). Although a larger number of axons seem to be affected by *Slit1* inactivation compared to the absence of *Robo1* and *Robo2*, it should be noted that *gfp*-expressing thalamic explants allow the visualization of all thalamic axons grown in the slice, in contrast to DiI tracings. Dotted lines indicate the borders of the explants and of the receiving slice.

(L) Quantification of (J) and (K). *p < 0.05, **p < 0.005, ***p < 0.001 by two-way ANOVA.

(M) Tracing of rostral TCAs in vivo at E16.5 in wild-type and $Slit1^{-/-}$ embryos. DiI crystals were placed into the rostral thalamus (rTh). After incubation, brains were cut horizontally to examine the trajectory of rostral axons in the subpallium.

(N and O) Wild-type rostral thalamic axons grow rostrally as a compact bundle (N; n = 13), whereas they disperse more in $Slit1^{-/-}$ brains (O; n = 9) as revealed by the measure of the width of the bundle within the subpallium "W" relative to the width at its entrance "w." Dotted lines indicate the borders of the DiI crystal injection site.

(P) Quantification of (N) and (O). ***p < 0.001 by Student's t test.

The following abbreviations are used: L, lateral; R, rostral. Scale bars represent 300 μm. Data in (H), (L), and (P) are presented as mean ± SEM.

rostral growth of Th1/2 axons was not modified by *Ntn1*-expressing COS cells in control or *Slit1* mutant host slices (Figures 4B and 4D; data not shown), they were strikingly attracted toward the source of Ntn1 when rSlit1 was added to the media (Figures 4C and 4D). These experiments reveal that Ntn1-attractive activity in the subpallium ex vivo requires Slit1 function. Furthermore, these results provide an explanation for the previously observed attractive activity of *Ntn1*-expressing cells grafted in the cerebral cortex [10] where high levels of *Slit1* are found [17].

To further determine the function of endogenous Ntn1 and Slit1 signaling in rostral TCA pathfinding, we first reanalyzed the phenotype of $Ntn1^{-/-}$ mutant embryos [10]. In the genetic background that we examined, retrograde and anterograde DiI tracings only revealed a mild dispersion of rostral axons in a very low percentage of $Ntn1^{-/-}$ embryos (2 of 35; Figure S4; data not shown). We nevertheless observed a small but significant shift of Th1/2 axons toward intermediate and caudal levels of the corridor when grown in $Ntn1^{-/-}$ slices (Figure S4). While consistent with the fact that $Ntn1^{-/-}$ embryos are hypomorphs [25] and show a variable phenotype in distinct genetic backgrounds, our results confirm that reducing *Ntn1* levels impairs the fine positioning of rostral axons ex vivo. Moreover, to determine whether Slit/Robo signaling is necessary to attract rostral TCAs, we performed similar coculture experiments in 45° corridor host slices in the absence of either Robo receptors or Slit1 (Figures 4E and 4I). Whereas wild-type Th1/2 axons grew rostrally in wild-type slices, axons lacking Robo1 and Robo2 receptors additionally grew at intermediate and caudal regions in the corridor (Figures 4F–4H). Similarly, a significant proportion of Th1/2 axons were dispersed toward intermediate and caudal levels when grown in $Slit1^{-/-}$ slices (Figures 4J–4L). Together, these experiments indicate that the lack of Slit1/Robo signaling ex vivo impairs the rostral channeling of Th1/2 axons, as expected if Slit1 participates in a rostral attractive signal. To test whether *Slit1* inactivation in vivo affects the positioning of rostral TCAs, we performed fine anterograde labeling of the rostral thalamus in $Slit1^{-/-}$ brains (Figures 4M–4P). We reproducibly observed that in the absence of Slit1, rostral thalamic axons dispersed more in the corridor compared to controls (Figure 4O), demonstrating that the fine positioning of Th1/2 axons requires Slit1 function. Overall, our results show that the combination of these two cues produces a strikingly nonlinear guidance activity, which provides precise spatial information for TCA navigation.

Conclusions

We have shown that TCA topography begins to be established within the corridor, where Slit1 has a dual role, acting as a rostral repellent to position intermediate axons while it enables Ntn1-mediated attraction to channel rostral axons. Although future experiments will address the mechanisms underlying these responses, our study reveals that combinations of guidance cues can trigger multiple and unexpected axonal behaviors depending on their relative concentrations, thereby producing the repertoire of responses necessary for the formation of complex axonal tracts.

Supplemental Information

Supplemental Information includes four figures, Supplemental Experimental Procedures, and three movies and can be found with this article online at doi:10.1016/j.cub.2011.09.008.

Acknowledgments

We are grateful to Kim Nguyen Ba-Charvet for advice and critical reading of the manuscript and to Alain Chedotal and Evelyne Bloch-Gallego for sharing mutant mouse colonies and scientific discussion. We thank Marc Ekker and Noel Ghanem for providing the *I56ii-LacZ* regulatory sequence and Eloisa Herrera, Valérie Castellani, Alessandra Pierani, and Xavier Morin for critically reading early versions of this paper. We are also grateful to members from the Garel and López-Bendito laboratories for stimulating discussions, ideas, and critical reading of the manuscript. This work was supported by grants from the INSERM "Avenir" program, the City of Paris, and the European Young Investigator (EURYI) program to S.G.; by Spanish Ministry of Science and Innovation grants BFU2006-00408/BFI and BFU2009-08261, Human Frontier Science Program research grant RGP29/2008, and CONSOLIDER grant CSD2007-00023 to G.L.-B.; and by the Program of Integrated Actions (PAI) Picasso to S.G. and G.L.-B. F.B. was supported by a fellowship from the French Ministry of Research and L.L. by a fellowship from the Association pour la Recherche sur le Cancer. P.M.-M. is supported by a Formación Personal Investigador fellowship from the Spanish Ministry of Science and Innovation. E.L.-D. is supported by a CONSOLIDER fellowship from the CSIC. S.G. is a EURYI awardee.

Received: April 4, 2011
Revised: July 12, 2011
Accepted: September 1, 2011
Published online: October 13, 2011

References

1. López-Bendito, G., and Molnár, Z. (2003). Thalamocortical development: how are we going to get there? Nat. Rev. Neurosci. *4*, 276–289.
2. Garel, S., and Rubenstein, J.L.R. (2004). Intermediate targets in formation of topographic projections: inputs from the thalamocortical system. Trends Neurosci. *27*, 533–539.
3. Vanderhaeghen, P., and Polleux, F. (2004). Developmental mechanisms patterning thalamocortical projections: intrinsic, extrinsic and in between. Trends Neurosci. *27*, 384–391.
4. López-Bendito, G., Cautinat, A., Sánchez, J.A., Bielle, F., Flames, N., Garratt, A.N., Talmage, D.A., Role, L.W., Charnay, P., Marín, O., and Garel, S. (2006). Tangential neuronal migration controls axon guidance: a role for neuregulin-1 in thalamocortical axon navigation. Cell *125*, 127–142.
5. Garel, S., Huffman, K.J., and Rubenstein, J.L.R. (2003). Molecular regionalization of the neocortex is disrupted in Fgf8 hypomorphic mutants. Development *130*, 1903–1914.
6. Garel, S., Yun, K., Grosschedl, R., and Rubenstein, J.L.R. (2002). The early topography of thalamocortical projections is shifted in Ebf1 and Dlx1/2 mutant mice. Development *129*, 5621–5634.
7. Piñon, M.C., Tuoc, T.C., Ashery-Padan, R., Molnár, Z., and Stoykova, A. (2008). Altered molecular regionalization and normal thalamocortical connections in cortex-specific Pax6 knock-out mice. J. Neurosci. *28*, 8724–8734.
8. Dufour, A., Seibt, J., Passante, L., Depaepe, V., Ciossek, T., Frisén, J., Kullander, K., Flanagan, J.G., Polleux, F., and Vanderhaeghen, P. (2003). Area specificity and topography of thalamocortical projections are controlled by ephrin/Eph genes. Neuron *39*, 453–465.
9. Wright, A.G., Demyanenko, G.P., Powell, A., Schachner, M., Enriquez-Barreto, L., Tran, T.S., Polleux, F., and Maness, P.F. (2007). Close homolog of L1 and neuropilin 1 mediate guidance of thalamocortical axons at the ventral telencephalon. J. Neurosci. *27*, 13667–13679.
10. Powell, A.W., Sassa, T., Wu, Y., Tessier-Lavigne, M., and Polleux, F. (2008). Topography of thalamic projections requires attractive and repulsive functions of Netrin-1 in the ventral telencephalon. PLoS Biol. *6*, e116.
11. Bonnin, A., Torii, M., Wang, L., Rakic, P., and Levitt, P. (2007). Serotonin modulates the response of embryonic thalamocortical axons to netrin-1. Nat. Neurosci. *10*, 588–597.
12. Bielle, F., Marcos-Mondejar, P., Keita, M., Mailhes, C., Verney, C., Nguyen Ba-Charvet, K., Tessier-Lavigne, M., Lopez-Bendito, G., and Garel, S. (2011). Slit2 activity in the migration of guidepost neurons shapes thalamic projections during development and evolution. Neuron *69*, 1085–1098.
13. Seibt, J., Schuurmans, C., Gradwhol, G., Dehay, C., Vanderhaeghen, P., Guillemot, F., and Polleux, F. (2003). Neurogenin2 specifies the

connectivity of thalamic neurons by controlling axon responsiveness to intermediate target cues. Neuron *39*, 439–452.

14. Zerucha, T., Stühmer, T., Hatch, G., Park, B.K., Long, Q., Yu, G., Gambarotta, A., Schultz, J.R., Rubenstein, J.L., and Ekker, M. (2000). A highly conserved enhancer in the Dlx5/Dlx6 intergenic region is the site of cross-regulatory interactions between Dlx genes in the embryonic forebrain. J. Neurosci. *20*, 709–721.
15. Ghanem, N., Yu, M., Poitras, L., Rubenstein, J.L., and Ekker, M. (2008). Characterization of a distinct subpopulation of striatal projection neurons expressing the Dlx genes in the basal ganglia through the activity of the I56ii enhancer. Dev. Biol. *322*, 415–424.
16. Bagri, A., Marín, O., Plump, A.S., Mak, J., Pleasure, S.J., Rubenstein, J.L.R., and Tessier-Lavigne, M. (2002). Slit proteins prevent midline crossing and determine the dorsoventral position of major axonal pathways in the mammalian forebrain. Neuron *33*, 233–248.
17. Marillat, V., Cases, O., Nguyen-Ba-Charvet, K.T., Tessier-Lavigne, M., Sotelo, C., and Chédotal, A. (2002). Spatiotemporal expression patterns of slit and robo genes in the rat brain. J. Comp. Neurol. *442*, 130–155.
18. Plump, A.S., Erskine, L., Sabatier, C., Brose, K., Epstein, C.J., Goodman, C.S., Mason, C.A., and Tessier-Lavigne, M. (2002). Slit1 and Slit2 cooperate to prevent premature midline crossing of retinal axons in the mouse visual system. Neuron *33*, 219–232.
19. Nguyen-Ba-Charvet, K.T., Di Meglio, T., Fouquet, C., and Chédotal, A. (2008). Robos and slits control the pathfinding and targeting of mouse olfactory sensory axons. J. Neurosci. *28*, 4244–4249.
20. López-Bendito, G., Flames, N., Ma, L., Fouquet, C., Di Meglio, T., Chedotal, A., Tessier-Lavigne, M., and Marín, O. (2007). Robo1 and Robo2 cooperate to control the guidance of major axonal tracts in the mammalian forebrain. J. Neurosci. *27*, 3395–3407.
21. Braisted, J.E., Ringstedt, T., and O'Leary, D.D.M. (2009). Slits are chemorepellents endogenous to hypothalamus and steer thalamocortical axons into ventral telencephalon. Cereb. Cortex *19* (*Suppl 1*), i144–i151.
22. Stein, E., and Tessier-Lavigne, M. (2001). Hierarchical organization of guidance receptors: silencing of netrin attraction by slit through a Robo/DCC receptor complex. Science *291*, 1928–1938.
23. Bai, G., Chivatakarn, O., Bonanomi, D., Lettieri, K., Franco, L., Xia, C., Stein, E., Ma, L., Lewcock, J.W., and Pfaff, S.L. (2011). Presenilin-dependent receptor processing is required for axon guidance. Cell *144*, 106–118.
24. Garbe, D.S., and Bashaw, G.J. (2007). Independent functions of Slit-Robo repulsion and Netrin-Frazzled attraction regulate axon crossing at the midline in Drosophila. J. Neurosci. *27*, 3584–3592.
25. Serafini, T., Colamarino, S.A., Leonardo, E.D., Wang, H., Beddington, R., Skarnes, W.C., and Tessier-Lavigne, M. (1996). Netrin-1 is required for commissural axon guidance in the developing vertebrate nervous system. Cell *87*, 1001–1014.
26. Ming, G., Song, H., Berninger, B., Inagaki, N., Tessier-Lavigne, M., and Poo, M. (1999). Phospholipase C-gamma and phosphoinositide 3-kinase mediate cytoplasmic signaling in nerve growth cone guidance. Neuron *23*, 139–148.
27. Ooashi, N., and Kamiguchi, H. (2009). The cell adhesion molecule L1 controls growth cone navigation via ankyrin(B)-dependent modulation of cyclic AMP. Neurosci. Res. *63*, 224–226.